

SUPPLEMENTARY INFORMATION

S1- Preparation and characterization of superconducting tip.

STM tips made of superconducting materials are widely used to increase the energy resolution in STS measurements beyond the thermal energy limit [25], [39]. Lead (Pb) and Niobium (Nb) are the most used materials, mainly for practical reasons as they are BCS superconductors with high critical temperature. SC STM tips are normally produced by either etching wire of the mentioned materials or by indenting W (or PtIr) tips into samples of the superconducting material of choice [25,38,40-42].

The material employed in this article for the superconducting (SC) tips is Niobium, a conventional s-wave superconductor with a bulk transition temperature T_c of 9.3 K and critical magnetic field of $B_c=0.198$ T. The STM tips were produced by electrochemical etching commercial (99.9% pure) polycrystalline Nb wire of 0.25mm width [49]. A length of 2mm of the wire was submerged into a 22% HCl solution and then etched by applying a 25Hz ac voltage of 16V between the wire and a counter electrode of graphite. Etched tips were mounted into a tip holder and transferred to the preparation chamber where they were sputtered for 5 hours at 3 keV in order to remove oxides and yield the widest possible gap.

The resulting SC tips have an average gap of $\Delta=1.05$ mV at 1.2 K, Fig. 1S(a), and are fully capable of attaining atomic resolution as shown in Fig. 1S(b) where both the atomic periodicity and the standing waves of Cu(111) are resolved.

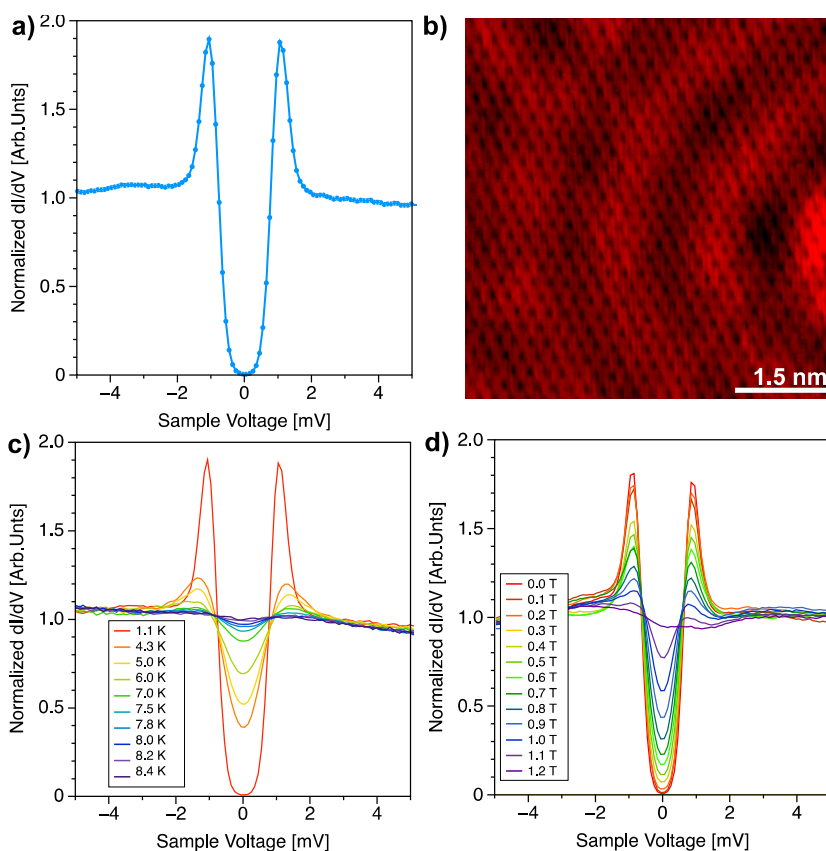


Figure S1. (a) Scanning tunnelling spectroscopy showing the Nb tip density of states at 1.2 K, $\Delta = 1.05$ mV calculated by fitting the spectra. STS parameters: $V=10$ mV, $I=2$ nA, $V_{mod}=100$ μ V. (b) STM image of Cu(111) single crystal showing routine atomic resolution and standing waves produced by a nearby defect. Image parameters: $V=10$ mV, $I=3$ nA, $T=1.2$ K. (c) Temperature

series: set of tunnelling spectra each recorded at a different temperature, the critical temperature is close to 8.4 K. STS parameters: $V=10$ mV, $I=2$ nA, $V_{mod}=100$ μ V. **(d)** Magnetic field series: tunnelling spectra of the Nb STM tip showing the evolution of the SC gap with increasing magnetic field at $T=1.2$ K, critical magnetic field close to 1.2 T. STS parameters: $V=10$ mV, $I=2$ nA, $V_{mod}=100$ μ V.

S2- Reversible functionalization

As already mentioned in the main text, the molecule can be released from the tip via voltage pulses above a certain threshold on molecule free areas. If the voltage pulse applied $\Delta V \geq +2$ V the functionalization of the tip may be reversed, this is depicted in Fig. S2(a) and (b). Here starting with a functionalized tip, blue spectrum, a voltage pulse of +2 V is applied over a given gr/Ir area of the sample (where the bias voltage is applied to the sample). The superconducting gap of the Nb tip is recovered, red spectrum, and some clusters that resemble the shape of a TCNQ are scanned over at the top right part of the STM image in Fig. 2S(b).

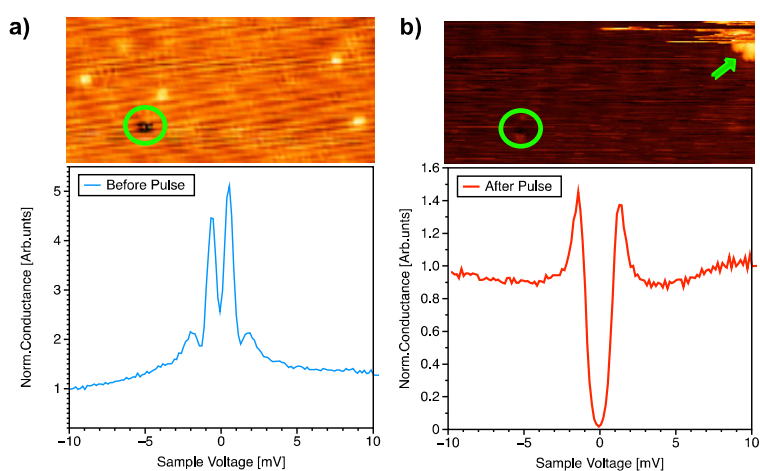


Figure S2. (a) STM topography image of a clean gr/Ir(111) area, where the spectrum of the TCNQ functionalized tip (blue) has been performed. Defect highlighted with green circle for reference. (b) STM topography image of the same clean gr/Ir(111) area after a +2 V pulse has been performed at the center of the image. The pulse is performed against the sample. STS performed after the voltage pulse shows that the pristine superconducting gap of the Nb tip is recovered. At the top of the STM image a TCNQ molecule maybe distinguished. Pulse parameters: $V=15$ mV, $I=0.5$ nA, $V=+2$ V and $t=100$ ms. Image parameters: $V=1$ V, $I=0.08$ nA, 20×20 nm. STS parameters: $V=10$ mV, $I=0.5$ nA, $V_{mod}=150$ μ V.

S3- Control experiment with un-functionalized Nb tip

This experiment is analogous to the ones presented in Fig. 2 and Fig. 3 of the main text, it is carried out over a gr/Ir area that is completely molecule free and the only difference is that in this case the tip is not functionalized with a TCNQ molecule. The experiment serves as a control experiment to confirm that if no molecule is present no sub-gap states will emerge no matter how close the tip is brought towards the sample, that in this case is 800 pm. As expected, no sub-gap state emerges throughout the whole length of the experiment, also no contact is stabilized between tip and sample in the sense that the current is always below the quantum of conductance G_0 .

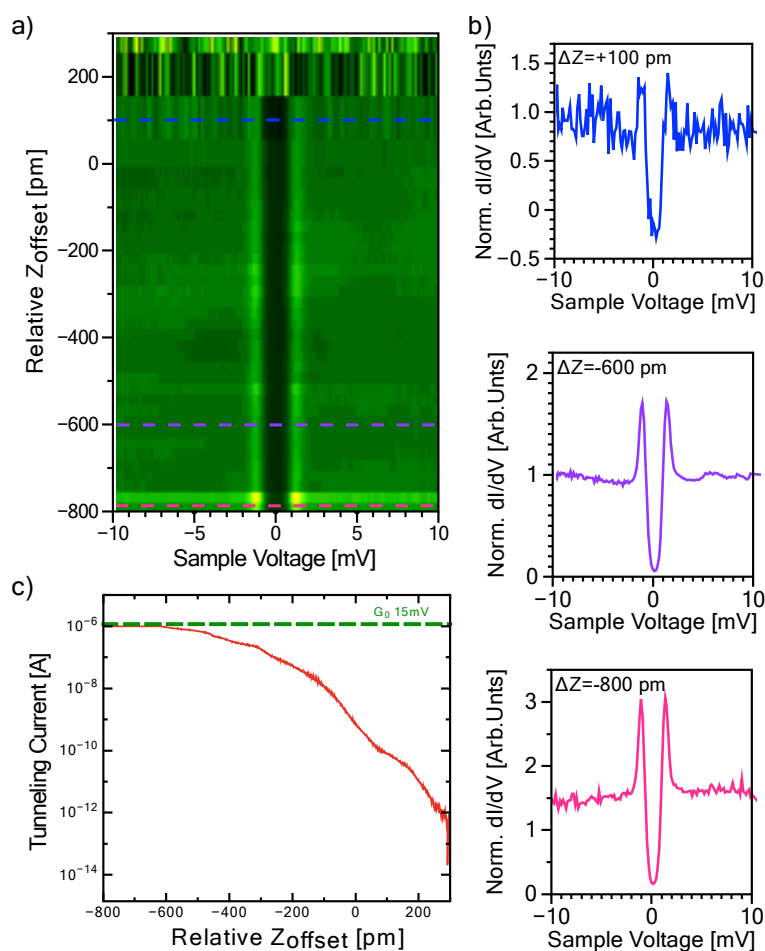


Figure S3. (a) Relative tip-sample distance dependence of STS spectra. The green-yellow colour scale represents the normalized dI/dV intensity as a function of bias voltage (horizontal axis) and relative tip-sample distances (vertical axis) of a non-functionalized Nb tip. The SC gap maybe observed throughout the whole experiment. Stabilization parameters throughout all the process: $V=15$ mV, $I=0.5$ nA, $V_{mod}=100$ μ V. (b) Three selected dI/dV spectra extracted from the stacked plot, each representative of the different regions in (a). (c) I vs Z curve acquired with the same

SC tip and covering the same 1100 pm Z offset range shown in (a). The conductance quantum, G_0 , is marked with a green dashed line. Stabilization parameters: $V=15$ mV, $I=0.5$ nA.

S4- Kondo fits from magnetic field series

Figure S4 shows the spectra of two Kondo resonances that correspond to the two functionalized tips depicted in Fig. 2 of the main manuscript when a magnetic field of 1.5 T is applied to quench the SC state of the Nb tip. Both spectra are fitted with the Fano function [35]:

$$\rho[E] = \frac{\left(q + \frac{E_0 - E}{\Gamma}\right)^2}{1 + \left(\frac{E_0 - E}{\Gamma}\right)^2}$$

Where q is the so-called asymmetry factor and Γ the intrinsic half width at half maximum (HWHM). The thermal broadening and the broadening produced by the lock-in modulation are accounted for by doing the convolution of the Fano function with the fermi function and with a semi-sphere [60]. Finally, to account for the broadening produced by the external magnetic field, the expected Zeeman splitting is subtracted from the value of HWHM. In the case of a magnetic impurity of spin $\frac{1}{2}$ the Zeeman splitting is given by [54].

$$2\Delta = 2(g\mu_B B S_{eff})$$

Where g is the Landé factor, μ_B is the Bohr magneton in electronvolts, B the magnetic field and S_{eff} the effective spin of the magnetic impurity. This yields a value of 0.14 meV in our case.

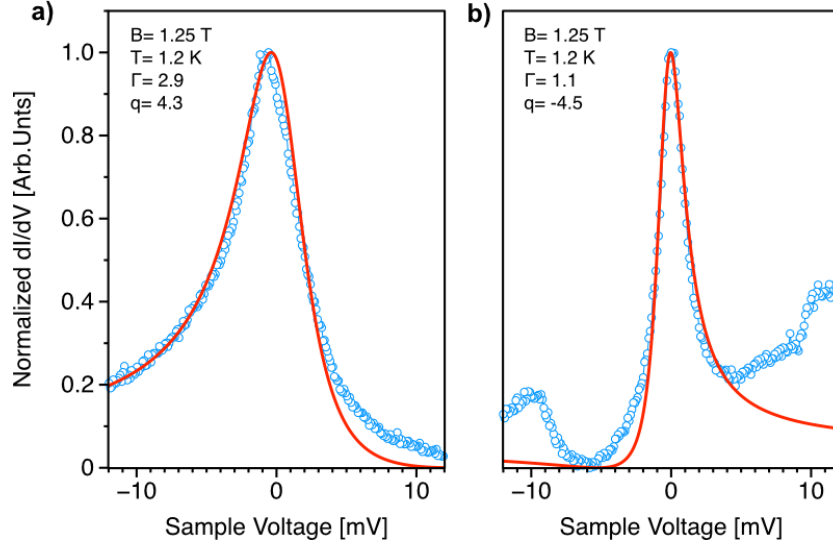


Figure S4. (a) Same tunnelling spectrum shown in Fig. 4(a) corresponding to a magnetic impurity in the strong coupling regime, the spectrum is fitted with a Fano function (red). Stabilization parameters: $V=15$ mV, $I=0.5$ nA, $V_{mod}=150$ μ V and $T=1.2$ K. (b) STS showing the Kondo resonance corresponding to the functionalized tip in the quantum phase (QP) transition shown in Fig. 4(b), the spectrum is also fitted with a Fano function shown in red. Stabilization parameters: $V=15$ mV, $I=0.5$ nA, $V_{mod}=150$ μ V and $T=1.2$ K

S5- Temperature evolution of Kondo resonances.

The temperature dependence of the intrinsic half width half maximum (HWHM) of two Kondo resonances are studied in the range from 1.2 K to ~ 17 K. For the lowest temperatures, a 1.5 T magnetic field was applied in order to quench the SC state of the tip, and the corresponding Zeeman splitting was accounted for, as explained in the previous section S4. However, note that the splitting always falls within the given error bar. The temperature evolution represented in green corresponds to the Kondo resonance of a TCNQ molecule in the strong coupling regime, in this case the data comes from a different functionalized tip that the one shown in the Fig.2 of the main text. The temperature dependence of the HWHM for the Kondo resonance represented in blue corresponds to a TCNQ molecule in the quantum phase (QP) transition, in this case this is the same functionalized tip as the one shown in the magnetic field series of Fig. 2 of the main text.

The intrinsic HWHM Γ is expected to be temperature dependent and broaden progressively with temperature, this is a signature of a Kondo system. In the case of finite temperatures its behaviour may be described by [14,16-18]:

$$\Gamma = \frac{1}{2} \sqrt{(\alpha k_B T)^2 + (2k_B T_K)^2}$$

Looking at this expression a linear growth is expected when $T \gg T_K$ with a slope given by α , a constant that depends on the system studied, for $T \ll T_K$ the width is expected to saturate ($\Gamma = k_B T_K$). Then the data presented in the graph below may be fitted with the above expression to calculate the Kondo temperature (T_K) for the magnetic impurities in the two coupling regimes. The calculated Kondo temperature for the magnetic impurity in the strong coupling regime is $T_K=23.8$ K ($\alpha=2.96$), in the case of the magnetic impurity in the QP transition $T_K=10.8$ K ($\alpha=1.65$).

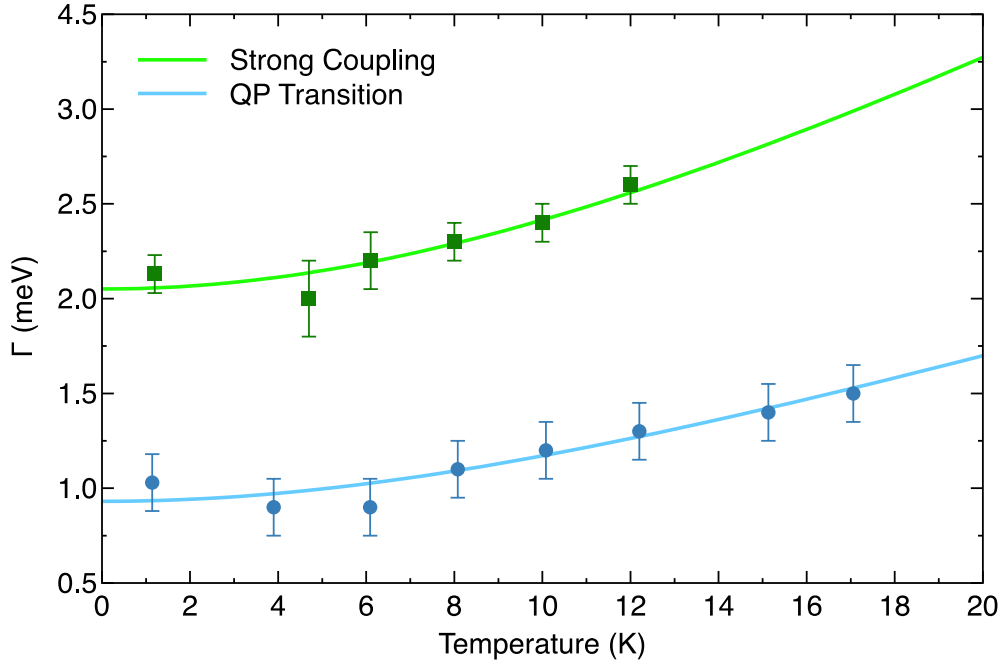


Figure S5. Intrinsic HWHM of the kondo resonances plotted against temperature. There are two sets of data for molecules in different coupling regimes, one in the strong coupling regime (green) and the other in the quantum phase transition (blue). Both sets of data show the expected evolution for the HWHM of a Kondo resonance with temperature, yielding a Kondo temperature T_K of 23.8 K and 10.8 K respectively.

S6- Relationship between the YSR and Kondo screening energy scale

Matsuura's universal relation describes the competition between the Kondo screening and the induced Yu-Shiba-Rushinov bound states. When a magnetic impurity is placed on a superconductor the spin of the magnetic impurity becomes under screened as there is a decrease in the number of itinerant electrons that can participate in the Kondo cloud. Matsuura predicted that the weaker the Kondo screening the more strongly bound the sub-gap states would be. Therefore, if the energy value of the sub-gap states (E_{BS}) is plotted against the energy of the Kondo screening channel ($k_B T_K$) the data should follow the relation predicted by Matsuura (green dashed line in Fig.S6) [30,31].

In order to complete the Matsuura plot, we need to know for the same functionalized tip: E_{BS} and $k_B T_K$. To calculate E_{BS} the spectra at $B=0$ T are fitted with a Cauchy function. The energy associated to the screening channel, $k_B T_K$, has been calculated by fitting the HWHM of the corresponding Kondo resonances ($B=1.5$ T) and then using the equation shown in section S5 when $T \rightarrow 0$ K [14,62]:

$$\Gamma_{T=0} = \frac{1}{2} \sqrt{4} k_B T_K = k_B T_K$$

In the case of the system studied in this work the QP transition occurs for a value of 0.99, that could seem to contradict the expected value of 0.3 reported on theoretical works [30,31] [62-65]. However, this deviation originates from the alternative definitions of T_K used in experimental and theoretical works, as pointed out in [25,29,61,62]. The most common expression for T_K used in theoretical works is [62-65]:

$$T_K = 0.29 \sqrt{U\Gamma} e^{\frac{\pi \varepsilon_x (\varepsilon_x + U)}{2\Gamma U}}$$

Where in this case T_K depends not only the hybridization value, but also on the energy position of the sub-gap states ε_x and on the Coulomb energy U . It is argued in refs [62] and [66] that the values of T_K calculated from this equation and the one used in this work may vary by a factor close to 4. Taking this into account, our result for the QP transition in Fig. S3 would be translated to a 0.25 ratio, which is in better agreement with the theoretical prediction of 0.3 corresponding to the alternative definition of T_K .

We propose to use both the external magnetic field and the procedure presented in this manuscript to modify the coupling regime of the magnetic impurity in combination as a new way to study Matsuura's universal relation. In principle the whole spectrum of the interaction strength of a magnetic molecule or adatom could be accessed by manipulating it onto a SC tip apex and performing spectroscopy experiments while changing the tip-sample distance (ΔZ). Then, an experiment could be envisioned like the ones presented in Fig. 2 and Fig. 3 of the main text but with the magnetic field turned on, in this way the width of the Kondo resonances (to calculate $k_B T_K$) that corresponds to the position all the E_{BS} for the different couplings of the magnetic impurity could be measured. Thus, covering the whole green curve presented in the figure below.

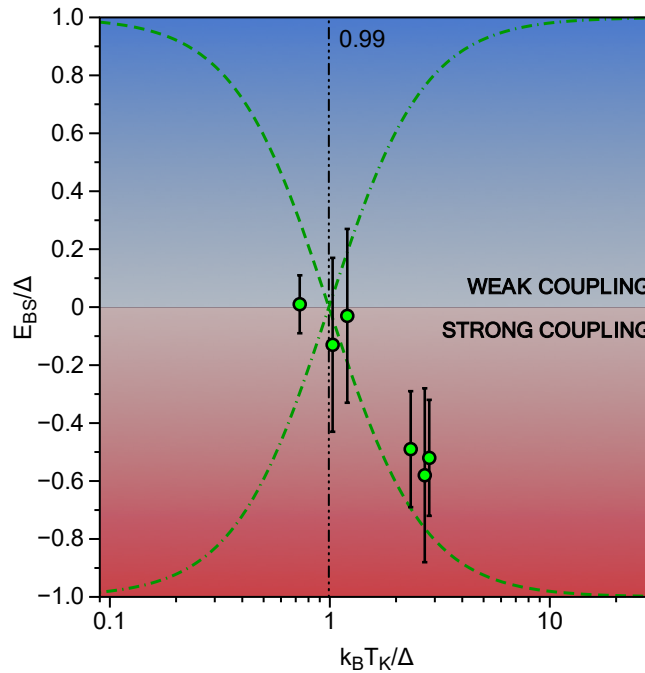


Figure S6. Relation between energy scales of the screening channel and magnetic induced bound states energy obtained at 1.2 K. E_{BS} is the position of the larger bound state, $E_{BS} < 0$ for a molecule in the strong coupling regime. The energy scale of the Kondo channel, $k_B T_K$, is

calculated by quenching the SC state of the tip with the external magnetic field and fitting the corresponding Kondo resonances with the Fano function.

S7- Reversibility of Z offset experiments

All the Z offset experiments presented in the manuscript are completely reversible. We ensured this by repeating each experiment back and forth several times, both the $I(Z)$ curves and the STS spectra. A selection of data demonstrating this is presented in figure S7 below.

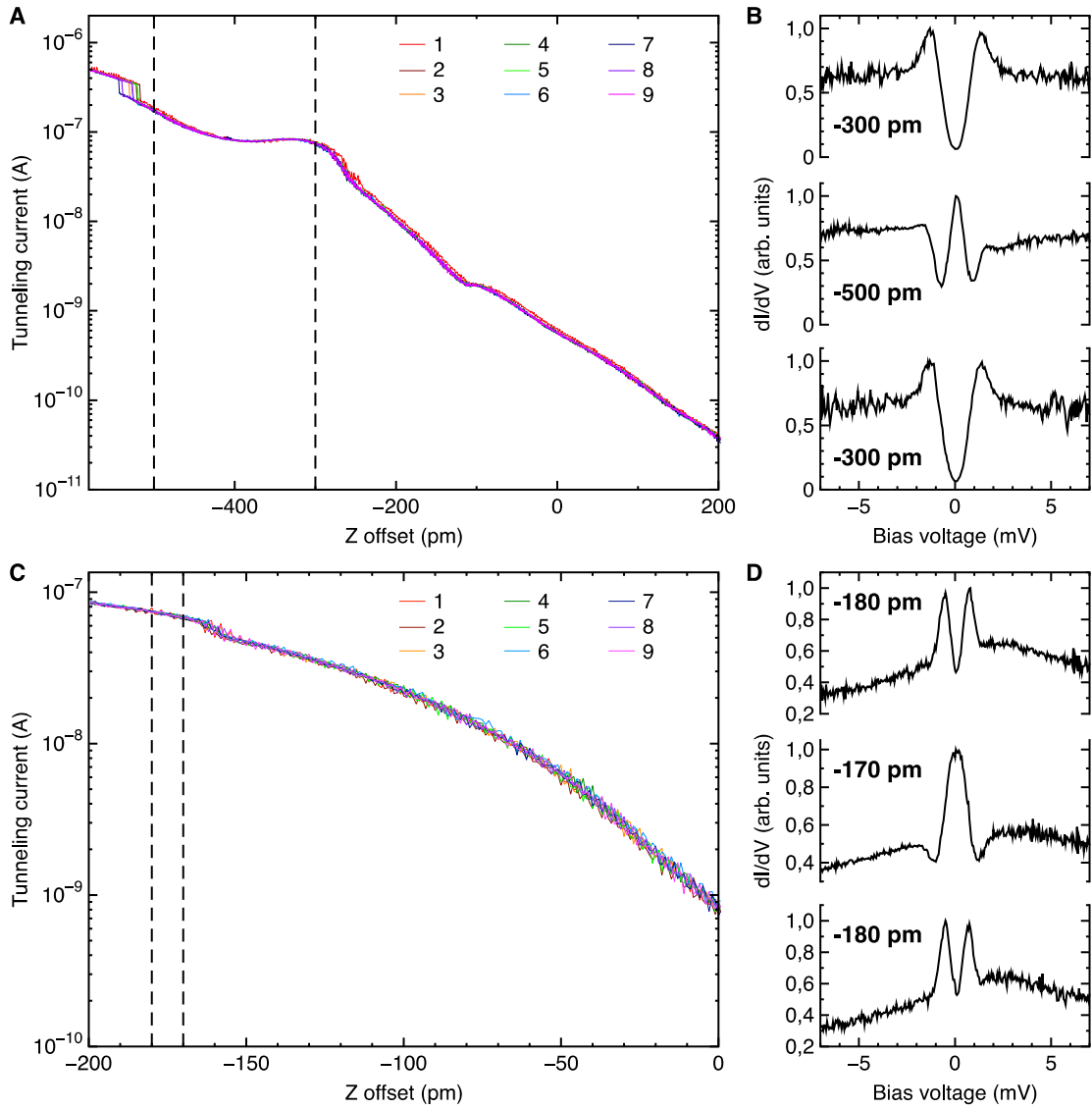


Figure S7. Reversibility in Z-offset experiments. Set of 9 consecutive $I(Z)$ curves corresponding to the experiments presented in figure 3 (panel A) and figure 4 (panel C) of the main text. Panels B and D show three consecutive STS spectra alternating between the two Z-offset values highlighted in panels A and C, respectively.